

Solution structure of human Ca²⁺-bound S100A12

Kuo-Wei Hung · Chan-Chia Hsu · Chin Yu

Received: 25 July 2013 / Accepted: 4 September 2013 / Published online: 22 September 2013
© Springer Science+Business Media Dordrecht 2013

Biological context

S100 proteins, named according to their solubility in 100 % ammonium sulfate, are low molecular weight Ca²⁺-binding proteins (9–13 kDa) solely found in vertebrates (Donato 2001). Currently, the S100 family constitutes more than 20 members that are expressed in several tissues and cell types for both intracellular and extracellular functions (Eckert et al. 2004). Most S100 proteins exist in their native conformation as homodimer through non-covalent interactions (Potts et al. 1995). Calcium binding is essential for S100 proteins adopting a conformation with hydrophobic regions exposed for regulating a wide range of important cellular processes via protein–protein interactions (Smith and Shaw 1998). S100 calcium-binding protein A12 (S100A12), also known as calgranulin C, expressed in neutrophils belongs to a subset of the S100 family elevated in the serum of patients with chronic inflammatory diseases (Foell et al. 2004; Guignard et al. 1995), including Kawasaki disease, Crohn's disease, atherosclerosis, rheumatoid arthritis and cystic fibrosis (Foell et al. 2007), and therefore has been considered as an emerging biomarker for the inflammatory response. According to the crystal structures, S100A12 exists as both dimer and hexamer in the presence of 200 mM CaCl₂ (Moroz et al. 2002). Zinc interactions can efficiently induce the hexamerization of Ca²⁺-loaded

S100A12 (Moroz et al. 2009a), which have been considered as an important oligomeric state for S100A12 binding targets (Xie et al. 2007). So far, two target proteins, including RAGE (Receptor for Advanced Glycation Endproducts) and SIP (Siah-1-interacting protein), have been reported interacting with human S100A12 (Filipek et al. 2002, Hofmann et al. 1999, Xie et al. 2007). However, most of studies are focus on the interaction of S100A12 with RAGE (Scheiber-Camoretti et al. 2013); it's still not clear whether the S100A12 protein in dimer form possesses specific-interaction with SIP. In the present study, we have accomplished the ¹H, ¹⁵N and ¹³C resonance assignments and determined the structure of human Ca²⁺-bound S100A12 dimer at low calcium concentration (5 mM) using a variety of NMR techniques. Moreover, comparisons between the solution and crystal structures of human S100A12 are described in detail in the present study.

Methods and results

Protein expression and purification

The recombinant human S100A12 composed of 92 amino acids was constructed into vector pET21b and expressed as protein without purification tag in *E. coli* BL21-CodonPlus. Isotopically ¹⁵N- and ¹⁵N/¹³C-labeled S100A12 proteins were prepared by growing *E. coli* in M9 minimal media, supplemented ¹⁵NH₄Cl and ¹²C₆-D-glucose or ¹³C₆-D-glucose. 0.5 mM isopropylthio-β-D-galactoside (IPTG) was added for the induction of protein expression, when the OD₆₀₀ of culture reached 0.6–0.8 at 37 °C. The culture with an additional 15 h incubation at 37 °C and 200 rpm shaking was harvested by centrifugation at 6,000 rpm and 4 °C for 20 min. The cell pellets were resuspended by pH

K.-W. Hung (✉)
Instrumentation Center, National Tsing Hua University,
Hsinchu, Taiwan, ROC
e-mail: kuowei@mx.nthu.edu.tw

C.-C. Hsu · C. Yu (✉)
Department of Chemistry, National Tsing Hua University,
Hsinchu, Taiwan, ROC
e-mail: cyu.nthu@gmail.com

8.0 buffer containing 20 mM Tris. The cell lysis was performed by using a French press. After 30 min of centrifugation at 16,000 rpm and 4 °C, the S100A12 protein expressed in soluble form was loaded onto a HiPrep 16/60 Q XL column (GE Healthcare) and purified with a linear gradient of 0–200 mM NaCl in pH 8.0 buffer. The fraction of elution was further purified by HiPrep 16/60 Phenyl FF column equilibrium with 50 mM Tris buffer (pH 7.5) containing 150 mM NaCl and 5 mM CaCl₂. The target protein was washed and eluted with buffers consisting of 50 mM Tris, 100 mM NaCl and 0–5 mM EDTA (pH 7.5). The protein with ~95 % purity was exchanged against pH 6.5 buffer (10 mM Hepes, 100 mM NaCl and 0.02 % (w/v) NaN₃) using a HiPrep 26/10 desalting column (GE Healthcare). The purity and identity of human S100A12 were first checked by SDS-PAGE analysis and then confirmed by ESI mass spectroscopy.

NMR spectroscopy

All NMR experiments were acquired at 37 °C on Varian NMR 700 MHz spectrometer equipped with triple resonance cryogenic probes. 1 mM of ¹⁵N and ¹⁵N/¹³C-labeled protein samples were prepared in 10 mM Hepes buffer (pH 6.5), 100 mM NaCl, 5 mM CaCl₂, 10 % D₂O and 0.02 % (w/v) NaN₃. Samples for the measurement of intermolecular NOEs were prepared by refolding of denatured ¹⁵N/¹³C-labeled and unlabeled S100A12 mixture at 1:1 molar ratio. Sequence specific assignments of the polypeptide backbone were made from ¹H–¹⁵N HSQC, HNCA, HN(CO)CA, HNCO, HN(CA)CO, CBCA(CO)NH and HNCACB spectra. Side chain resonances were assigned from the combined information content of the ¹⁵N-edited NOESY-HSQC, ¹H–¹³C HSQC, ¹³C-edited NOESY-HSQC, HCCH-TOCSY and HBHA(CO)NH. All NMR signals were referenced to ¹H resonance of the 2,2-dimethyl-2-silapentane-5-sulfonate. All 3D NOE experiments were acquired with a mixing time of 150 ms. NMR data were processed using software VnmrJ and analyzed by software SPARKY (T. D. Goddard and D. G. Kneller, SPARKY 3.114, University of California, San Francisco).

Structure calculation

The solution structures of S100A12 dimer were calculated by software ARIA 2.3 employing C2 symmetry parameters with a simulated annealing (SA) approach and then followed by a refinement procedure (Rieping et al. 2007). The NOE distance restraints applied for structure determination were extracted from ¹⁵N-edited NOESY-HSQC, ¹³C-edited NOESY-HSQC and ¹³C F1-filtered, F3-edited NOESY-HSQC spectra. The angle restraints including phi (φ) and psi (ψ) torsion angles of protein backbone were predicted

empirically using the TALOS software program (Cornilescu et al. 1999). Hydrogen-bonds were introduced as a pair of distance restraints based on NOE analysis in combination with the prediction of protein secondary structural elements using software CSI (Wishart and Sykes 1994). Non-bonded interactions were calculated by PARALLHDG force field. Torsion angle dynamics (TAD) was employed for the energy minimization in structure calculation. The initial-folded structures of dimeric protein were generated based on manually-assigned intramolecular and intermolecular NOEs. The unambiguous and ambiguous NOE restraints derived from outputs of previous ARIA run were analyzed and utilized as inputs for the next structure calculation. Lower ambiguous cutoff parameters and slow-cooling standard SA protocols were used in refinement steps of structure calculations. The structures with lowest overall energies were further calculated followed by water refinement in ARIA. The quality of calculated conformers was checked by analyzing the violations using MOLMOL and PROCHECK software programs (Koradi et al. 1996; Laskowski et al. 1996).

Structure determination of human S100A12

The molecular state of recombinant human S100A12 was identified as dimer in solution (Xie et al. 2007). The ¹⁵N–¹H HSQC spectra of human S100A12 at pH 6.5 contain a single set of well-dispersed NMR resonances, indicating that the S100A12 protein forming homodimer is well-structured (red peaks in Fig. 1a). Addition of 5 mM EDTA results in a significant chemical-shift change of ¹⁵N–¹H signals (blue peaks in Fig. 1a), suggesting that the purified S100A12 protein adopts a different conformation in the presence of calcium. The ¹H, ¹⁵N and ¹³C resonances of human Ca²⁺-S100A12 at pH 6.5 and 37 °C have been completely assigned and deposited in the BMRB under accession number 19293.

The solution structure of Ca²⁺-loaded S100A12 dimer was calculated with 2,169 experimental and empirical NMR restraints, including 1,989 NOE distance restraints, 36 hydrogen-bond distance restraints and 144 dihedral angle restraints, based on the distance geometry and energy minimization approaches used in ARIA-CNS. The superimposition of backbone traces for the ensemble of 20 lowest energy conformers selected from 200 calculated structures is shown in Fig. 1b, revealing a good agreement among applied NMR restraints. Table 1 shows a summary of structure statistics for the human Ca²⁺-bound S100A12 dimer. The root-mean-square-deviation (RMSD) values for the backbone atoms in structured regions and whole protein of 20 best structures were calculated to be 0.48 ± 0.12 and 1.46 ± 0.33 Å, respectively. The large RMSD of full-length protein is mainly due to the poorly defined loop

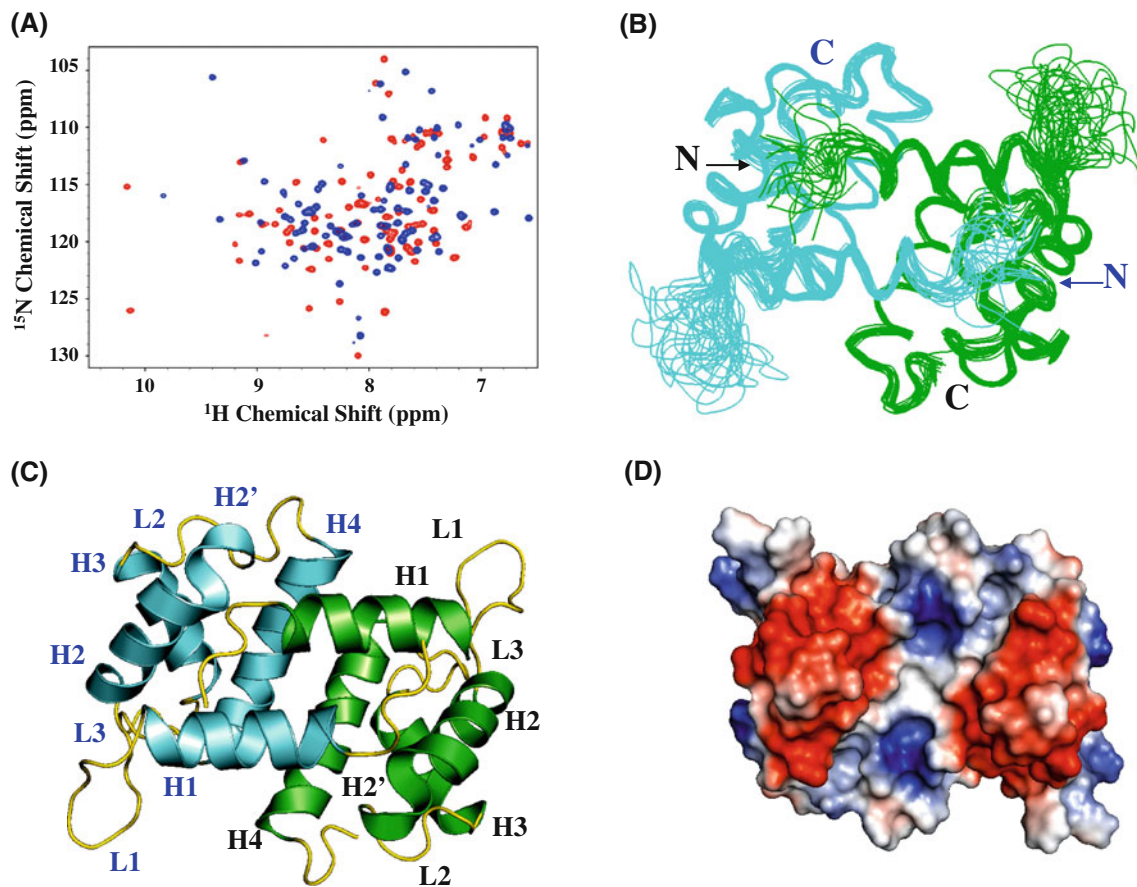


Fig. 1 **a** ^1H - ^{15}N HSQC spectra of Ca^{2+} -loaded S100A12 without (red) and with (blue) 5 mM EDTA acquired at pH 6.5 and 37 °C. **b** Superimposition of the backbone atoms of 20 final structures for the human Ca^{2+} -S100A12 dimer (green and cyan). The N- and C-terminal ends of subunits in green and cyan are labeled in black and blue, respectively. **c** Ribbon representation of the tertiary structure of human Ca^{2+} -S100A12 dimer. The secondary structure elements are

labeled using the same color codes in (b). Loops connecting H1–H2, H3–H4 and EF hands are labeled as L1, L3 and L2, respectively. **d** Surface charge distribution of human Ca^{2+} -S100A12 dimer shown as a 180° rotation of the view in (c). The surfaces with negative charge, positive charge and hydrophobic are colored in red, blue and white, respectively

regions in human Ca^{2+} -S100A12 dimer. The Ramachandran plot analysis shows that 80.2 % of residues are in the most favored region, 17.4 % in the additionally allowed region, 1.2 % in the generously allowed region and 1.2 % of residues are in the disallowed regions. The residues located in the disallowed regions of Ramachandran plot are due to lack of dihedral angle restraints during the structure determination. The NMR restraints and coordinates of 20 best structures of the S100A12 dimer have been deposited in the Protein Data Bank with ID 2M9G.

Overview of the solution structure of human Ca^{2+} -bound S100A12 dimer

The NMR structures of human S100A12 adopt a dimeric conformation in solution (Fig. 1b). 29 residues in protomer are involved in the dimer interface with an area of 1,525 Å², encompassing 8 hydrogen bonds and 304 non-

bonded contacts. Each subunit comprises four α -helices (H1, a.a. 6–18; H2, a.a. 30–41; H3, a.a. 51–61; and H4, a.a. 71–87) and one helix-like segment (H2', a.a. 42–44) in a H1–H2–H2'–H3–H4 topology (Fig. 1c) and two EF-hand motifs (EF-1 and EF-2) connected by loop L2, the so-called “hinge” region (Fig. 1c). Compare to the crystal structure of S100A12 determined with 200 mM CaCl_2 (PDB ID: 1E8A, Fig. 2a) (Moroz et al. 2001), the solution structures of S100A12 retain a similar structural fold with 1.12 Å of backbone RMSD (Table 2), revealing an “open” conformation between helices H3 and H4 with interhelical angles $\theta = 53.7^\circ$ and $\varphi = -102.9^\circ$ smaller than those found in PDB 1E8A ($\theta = 55.6^\circ$ and $\varphi = -108.7^\circ$, Table 2). Moreover, in our structure, an additional short helix-like segment H2', the extension of helix H2 with kink, was observed forming in loop L2, possibly due to the hydrophobic interactions between the hinge region and helix H4 composed of residues Leu⁴¹, Ile⁴⁵, Ile⁸⁰, Ala⁸¹ and Ala⁸⁴. A

Table 1 Structural statistics of human calcium-bound S100A12

Number of NMR restraints per protomer	
Intraresidual NOEs ($ i - j = 0$)	342
Sequential NOEs ($ i - j = 1$)	230
Short-range NOEs ($ 3 \geq i - j \geq 2 $)	173
Medium-range NOEs ($ 5 \geq i - j \geq 4 $)	69
Long-range NOEs ($ i - j > 5$)	103
Intermolecular NOEs	68
Hydrogen bonds	36
Dihedral angles	144
CNS energies (kcal mol ⁻¹) ^a	
E_{total}	$-6,499.39 \pm 268.33$
E_{bond}	50.57 ± 3.17
E_{angle}	287.28 ± 19.41
E_{impr}	501.72 ± 56.45
E_{dihed}	957.98 ± 11.17
E_{vdw}	-866.03 ± 32.75
E_{elec}	$-7,430.92 \pm 266.58$
R.M.S.D. from experimental constraints	
Distances (Å)	0.037 ± 0.010
Dihedral angles (deg.)	1.09 ± 0.10
R.M.S.D. from mean structure	
Backbone in structured region (Å) ^b	0.48 ± 0.12
Heavy atoms in structured region (Å) ^b	0.98 ± 0.10
Backbone in whole protein (Å)	1.46 ± 0.33
Heavy atoms in whole protein (Å)	2.16 ± 0.28
Ramachandran plot	
Most favored region (%)	80.2
Additionally allowed (%)	17.4
Generously allowed (%)	1.2
Disallowed (%)	1.2

^a The NOE and dihedral angle potentials were calculated with force constants of 50 kcal mol⁻¹ Å⁻² and 200 kcal mol⁻¹ rad⁻², respectively

^b Residues in the structured regions: 6–18, 30–44, 51–61, 71–87

similar result was also found in the X-ray structure of Ca²⁺-free S100A12 (PDB ID: 2WCE, Fig. 2b) (Moroz et al. 2009a), which has a 2.56 Å backbone RMSD to the solution structure and forms a longer H2' (a.a. 42–48) by extended hydrophobic contacts among residues Leu⁴¹, Ile⁴⁸, Ala⁸¹, Ala⁸⁴ and Ala⁸⁵ due to a “closed” conformation with $\theta = 19.4^\circ$ and $\varphi = 128.5^\circ$ between helices H3 and H4 (Table 2). Furthermore, the C-terminal loop (His⁸⁸–Glu⁹²) invisible in PDB 1E8A adopts an orientation in contact with the hinge region and helix H4 in the NMR solution structure (Fig. 2a), which blocks the active sites in S100 proteins, revealing an “incompletely open” conformation for the S100A12 protein at low calcium concentration (5 mM). Interestingly, the crystal structures of Zn²⁺ and Ca²⁺/Cu²⁺-bound S100A12 (PDB ID: 2WCB and 1ODB, Fig. 2c, d) (Moroz et al. 2003, Moroz et al. 2009a),

which show 1.79 and 1.30 Å backbone RMSDs to the NMR structure, respectively (Table 2), indicate that zinc and copper share the same binding site on human S100A12 and their interactions are able to reorient the C-terminal loops of both apo- and Ca²⁺-loaded S100A12 and extend the length of helix H4 from His⁸⁸ to His⁹⁰. Our data, together with the results reported previously, suggest that zinc/copper interactions lead to the Ca²⁺-loaded S100A12 adopting a “completely open” structure with larger interhelical angles between helices H3 and H4 ($\theta = 57.6^\circ$ and $\varphi = -106.4^\circ$, Table 2) for target recognition. In contrast to the contribution of Zn²⁺-induced hexamerization of Ca²⁺-S100A12 to binding to RAGE (Moroz et al. 2009b), our finding raises the possibility that the Zn²⁺/Cu²⁺-induced conformation changes, which move the C-terminal loop from blocking the target-binding sites in Ca²⁺-S100A12 and extend the length of helix H4, could also play an important role in the enhancement of binding affinity to the target protein RAGE.

In addition, the results of amino-acid alignment indicate that the side chains of residues involved in the calcium binding of human S100A12, including Glu³² in EF-1 and Asp⁶², Asn⁶⁴, Asp⁶⁶ and Glu⁷³ in EF-2, are well-conserved among six mammalian species with sequence identity from 64 to 73 % (Fig. 2e). In contrast to the Ca²⁺-binding loop (L3) in EF-2, loop L1 lacks negatively charged surfaces for the calcium coordination in EF-1 (Fig. 1d), which mainly consists of the backbone carbonyl groups of Ser¹⁹, Lys²², His²⁴ and Thr²⁷ with a single acidic residue Glu³². Interestingly, in conjunction with the data reported in Xie et al. (2007), addition of 5 mM CaCl₂ to apo-S100A12 results in the ¹H–¹⁵N HSQC cross-peaks corresponding to segments Met¹–Glu⁶ and Ser¹⁹–Ser²⁹ line-broadening and poorly defined in the solution structures of S100A12 with large RMSD values (1.77 ± 0.60 and 2.64 ± 0.76 Å, respectively), implying that the calcium binding process in EF-1 occurs on an intermediate NMR timescale. Our data report for the first time that the interaction of calcium at low concentrations can considerably increase the flexibility of the N-terminal regions of S100A12 with a shorter helix H1, which are putative binding sites for S100 targets. Furthermore, our finding also suggests that the EF-1 motif of S100A12 possesses a much weaker Ca²⁺-binding affinity than EF-2, confirming the reported results (Dell'Angelica et al. 1994).

Interestingly, the zinc coordination by conserved residues His¹⁶, Asp²⁶, His⁸⁶ and His⁹⁰ between protomers of S100A12 could result in an enhancement of Ca²⁺-binding affinity by 1,500 folds (Dell'Angelica et al. 1994). However, the mechanism is not clear so far. In the present study, the solution structures of S100A12 reveal that the flexible Ca²⁺-binding loop in EF-1 might be stabilized by the zinc interaction with residue Asp²⁶, as the observation

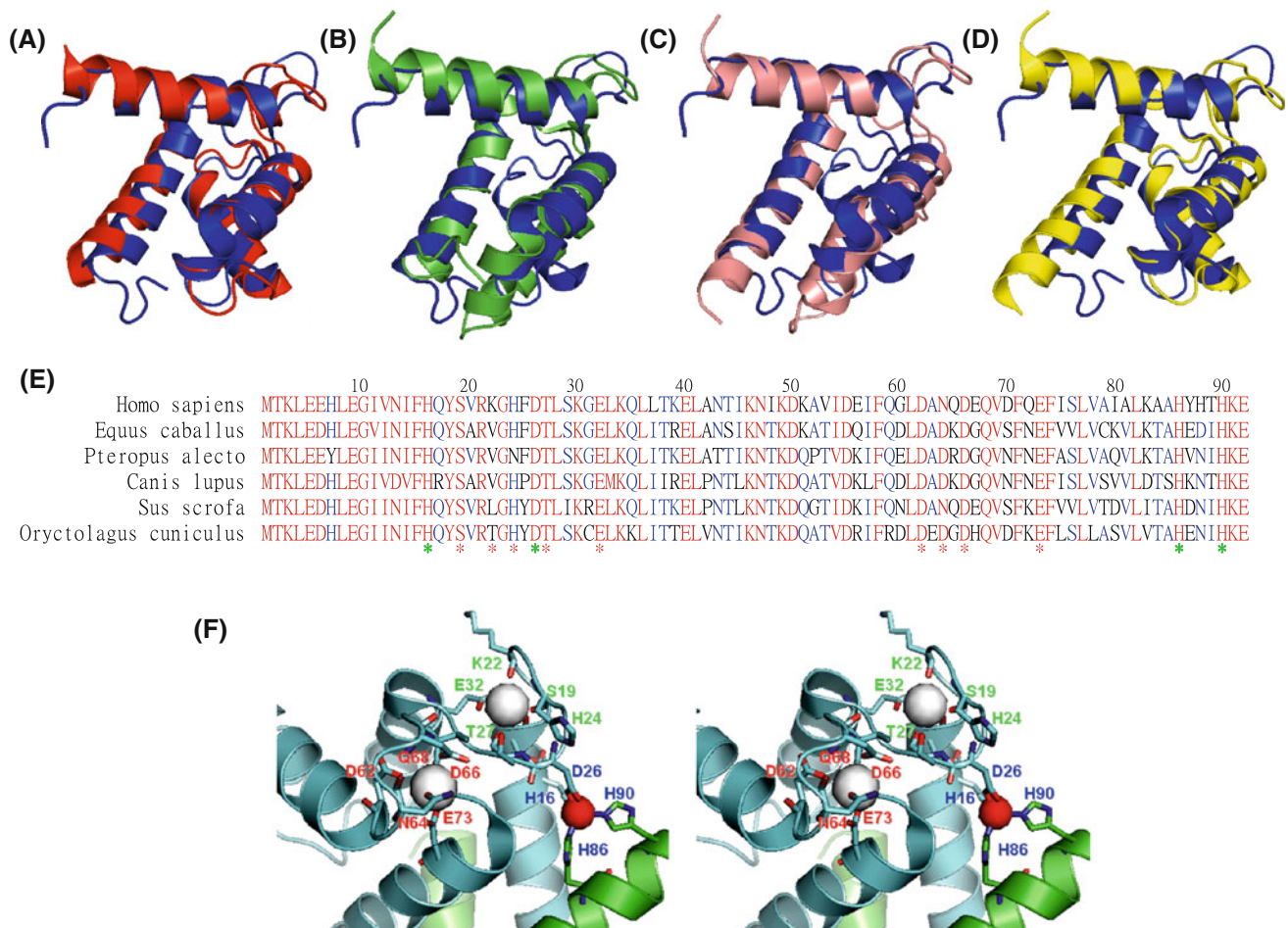


Fig. 2 **a** Comparison of the solution structure of human S100A12 (blue) with the X-ray crystal structures in Ca^{2+} -bound form (red, PDB ID: 1E8A), **b** Ca^{2+} -free form (green, PDB ID: 2WCE), **c** Zn^{2+} -bound form (violet, PDB ID: 2WCB) and **d** $\text{Ca}^{2+}/\text{Cu}^{2+}$ -bound form (yellow, PDB ID: 1ODB). The results show that the solution structure of human S100A12 dimer adopts an “incompletely open” conformation and further zinc/copper interactions result in a completely “open” structure formation. **e** Amino acid sequence alignments of

proteins in S100A12 family. The identities/similarities of S100A12 are scaled from 73/85 to 64/82 %. Residues involved in calcium and zinc/copper coordination of human S100A12 are marked with red and green asterisks, respectively, revealing well-conserved metal-binding sites for function. **f** Close-up stereo view of the metal-binding sites found in PDB 1ODB. The Ca^{2+} -binding residues in EF-1 and EF-2 are labeled green and red, respectively. Residues labeled in blue represent the $\text{Cu}^{2+}/\text{Zn}^{2+}$ -binding sites between protomers

Table 2 Comparison of the solution and crystal structures of human S100A12

Protein state	EF-2 angles ^a			Backbone RMSD to PDB 2M9G (Å)
	N-terminal coordinate of second helix			
		θ (°)	φ (°)	
Ca^{2+} -bound form ^b	-8.087, -0.993, -5.792	53.747	-102.932	–
Ca^{2+} -bound form ^c	-8.368, -2.881, -6.657	55.633	-108.740	1.16
Apo form ^d	8.978, -10.700, -1.206	19.397	128.505	2.56
Zn^{2+} -bound form ^e	-8.601, 4.383, -4.643	18.195	93.680	1.79
$\text{Ca}^{2+}/\text{Cu}^{2+}$ -bound form ^f	-9.002, -4.198, -5.784	57.552	-106.412	1.30

^a The EF-hand angles between helices H3 and H4 in S100A12 were calculated by the Vector Geometry Mapping (VGM) program using PDB 1DMO as reference structure (Yap et al. 2002)

^b PDB ID: 2M9G

^c PDB ID: 1E8A

^d PDB ID: 2WCE

^e PDB ID: 2WCB

^f PDB ID: 1ODB

shown in Fig. 2f, which is located at loop L1 forming a regulating link between the functions of S100A12 binding to zinc/copper and calcium. However, how zinc/copper interactions alter the function of Ca²⁺-S100A12 binding to various targets remain open questions.

Acknowledgments This work was supported by grants from the National Science Council of the Republic of China (NSC 102-2731-M-007-002-MY2 to K.W. Hung and NSC 100-2113-M-007-012-MY3 to C. Yu). The NMR spectra were obtained at the Instrumentation Center at National Tsing Hua University (NTHU) supported by NSC of Taiwan.

References

- Cornilescu G, Delaglio F, Bax A (1999) Protein backbone angle restraints from searching a database for chemical shift and sequence homology. *J Biomol NMR* 13(3):289–302
- Dell'Angelica EC, Schleicher CH, Santome JA (1994) Primary structure and binding properties of calgranulin C, a novel S100-like calcium-binding protein from pig granulocytes. *J Biol Chem* 269(46):28929–28936
- Donato R (2001) S100: a multigenic family of calcium-modulated proteins of the EF-hand type with intracellular and extracellular functional roles. *Int J Biochem Cell Biol* 33(7):637–668
- Eckert RL, Broome AM, Ruse M, Robinson N, Ryan D, Lee K (2004) S100 proteins in the epidermis. *J Invest Dermatol* 123(1):23–33
- Filipek A, Jastrzebska B, Nowotny M, Kuznicki J (2002) CacyBP/SIP, a calcyclin and Siah-1-interacting protein, binds EF-hand proteins of the S100 family. *J Biol Chem* 277(32):28848–28852
- Foell D, Frosch M, Sorg C, Roth J (2004) Phagocyte-specific calcium-binding S100 proteins as clinical laboratory markers of inflammation. *Clinica Chimica Acta* 344(1–2):37–51
- Foell D, Wittkowski H, Vogl T, Roth J (2007) S100 proteins expressed in phagocytes: a novel group of damage-associated molecular pattern molecules. *J Leukoc Biol* 81(1):28–37
- Guignard F, Muel J, Markert M (1995) Identification and characterization of a novel human neutrophil protein related to the S100 family. *Biochem J* 309(Pt 2):395–401
- Hofmann MA, Drury S, Fu C, Qu W, Taguchi A, Lu Y, Avila C, Kambham N, Bierhaus A, Nawroth P, Neurath MF, Slattey T, Beach D, McClary J, Nagashima M, Morser J, Stern D, Schmidt AM (1999) RAGE mediates a novel proinflammatory axis: a central cell surface receptor for S100/calgranulin polypeptides. *Cell* 97(7):889–901
- Koradi R, Billeter M, Wuthrich K (1996) MOLMOL: a program for display and analysis of macromolecular structures. *J Mol Grap* 14(1):51–55, 29–32
- Laskowski RA, Rullmann JA, MacArthur MW, Kaptein R, Thornton JM (1996) AQUA and PROCHECK-NMR: programs for checking the quality of protein structures solved by NMR. *J Biomol NMR* 8(4):477–486
- Moroz OV, Antson AA, Murshudov GN, Maitland NJ, Dodson GG, Wilson KS, Skibshoj I, Lukanidin EM, Bronstein IB (2001) The three-dimensional structure of human S100A12. *Acta Crystallogr Sect D: Biol Crystallogr* 57(Pt 1):20–29
- Moroz OV, Antson AA, Dodson EJ, Burrell HJ, Grist SJ, Lloyd RM, Maitland NJ, Dodson GG, Wilson KS, Lukanidin E, Bronstein IB (2002) The structure of S100A12 in a hexameric form and its proposed role in receptor signalling. *Acta Crystallogr Sect D: Biol Crystallogr* 58(Pt 3):407–413
- Moroz OV, Antson AA, Grist SJ, Maitland NJ, Dodson GG, Wilson KS, Lukanidin E, Bronstein IB (2003) Structure of the human S100A12-copper complex: implications for host-parasite defence. *Acta Crystallogr Sect D: Biol Crystallogr* 59(Pt 5):859–867
- Moroz OV, Blagova EV, Wilkinson AJ, Wilson KS, Bronstein IB (2009a) The crystal structures of human S100A12 in apo form and in complex with zinc: new insights into S100A12 oligomerisation. *J Mol Biol* 391(3):536–551
- Moroz OV, Burkitt W, Wittkowski H, He W, Ianoul A, Novitskaya V, Xie J, Polyakova O, Lednev IK, Shekhtman A, Derrick PJ, Bjoerk P, Foell D, Bronstein IB (2009b) Both Ca²⁺ and Zn²⁺ are essential for S100A12 protein oligomerization and function. *BMC Biochem* 10:11
- Potts BC, Smith J, Akke M, Macke TJ, Okazaki K, Hidaka H, Case DA, Chazin WJ (1995) The structure of calcyclin reveals a novel homodimeric fold for S100 Ca(2+)-binding proteins. *Nat Struct Biol* 2(9):790–796
- Rieping W, Habeck M, Bardiaux B, Bernard A, Malliavin TE, Nilges M (2007) ARIA2: automated NOE assignment and data integration in NMR structure calculation. *Bioinformatics* 23(3):381–382
- Scheiber-Camoretti R, Mehrotra A, Yan L, Raman J, Beshai JF, Hofmann Bowman MA (2013) Elevated S100A12 and sRAGE are associated with increased length of hospitalization after non-urgent coronary artery bypass grafting surgery. *Am J Cardiovas Dis* 3(2):85–90
- Smith SP, Shaw GS (1998) A change-in-hand mechanism for S100 signalling. *Biochemistry and cell biology. Biochimie et biologie cellulaire* 76(2–3):324–333
- Wishart DS, Sykes BD (1994) The 13C chemical-shift index: a simple method for the identification of protein secondary structure using 13C chemical-shift data. *J Biomol NMR* 4(2):171–180
- Xie J, Burz DS, He W, Bronstein IB, Lednev I, Shekhtman A (2007) Hexameric calgranulin C (S100A12) binds to the receptor for advanced glycated end products (RAGE) using symmetric hydrophobic target-binding patches. *J Biol Chem* 282(6):4218–4231
- Yap KL, Ames JB, Swindells MB, Ikura M (2002) Vector geometry mapping. A method to characterize the conformation of helix-loop-helix calcium-binding proteins. *Methods Mol Biol* 173:317–324